Academic Journal of Environment & Earth Science
ISSN 2616-5872 Vol.4, Issue 7: 49-55, DOI: 10.25236/AJEE.2022.040709

Grand Canonical Studies on the Hydrogen Evolution Mechanism of Two-dimensional 1T Phase MoS_2

Yi An[1,*]

[1]*Siyuan Laboratory, Department of Physics, Jinan University, Guangzhou, Guangdong, 510632, China*
**Corresponding author: edithan@stu2019.jnu.edu.cn*

Abstract: *Electrolyzing water is one of the most common ways to obtain hydrogen in current research, and hydrogen evolution reaction (HER) occurs at the cathode during the process of electrolysis of water. Platinum (Pt) is currently recognized as the best HER catalyst. However, the high cost of Pt limits its widespread application. As an alternative to Pt, 1T'-MoS_2 has received the most attention. Density Functional Theory (DFT) is widely used in HER reaction mechanism analysis, in the previous research, the catalyst system defaults to be electrical neutral. However, the charge is in a state of dynamics equilibrium in the actual reaction which results in the surface charge effects can only be captured under grand-canonical ensemble. In this work, we have demonstrated that the surface charges have a large impact on both HER thermodynamics and dynamics by grand-canonical calculations.*

Keywords: *1T'-MoS_2, Hydrogen evolution reaction, Reaction mechanism, First-principle, Grand-canonical calculations*

1. Introduction

With the growing energy shortage and environmental pollution, one of the most important challenges today is to establish a global-scale sustainable energy system for the future while protecting the environment[1-3]. Hydrogen can be used in fuel cells to generate clean electricity, an important method for hydrogen production is the electrolysis of water under acidic conditions by generating electricity from renewable energy sources such as solar and wind energy[4-6], Hydrogen evolution reaction (HER) is a cathodic reaction in the process of electrolysis of water, and HER may occur through the Volmer-Heyrovsky or Volmer-Tafel pathway, the Volmer reaction is the adsorption step, and the Heyrovsky/Tafel reaction is the desorption step[7]. Density Functional Theory (DFT) is widely used in HER catalytic reaction research[8-10]. According to the Sabatier principle, the HER exchange current density of the catalyst has a volcanic relationship with its hydrogen adsorption energy (ΔG_H) calculated by DFT[11-13], and $\Delta G_H \approx 0$ is a necessary condition for the catalyst to have good catalytic activity[14, 15]. Platinum (Pt) is currently recognized as the best HER catalyst. However, the high cost of Pt limits its wide application [14, 16-18], and the search for new and low-cost alternatives has become an urgent need in the current energy and catalysis fields. Understanding the HER reaction mechanism at the atomic and electronic levels is the key to designing new catalysts [19-23].

In the previous DFT calculation, in order to simplify the calculation, it is usually assumed that the catalyst is charge-neutral. Therefore, as the reaction proceeds, the Fermi level (E_F) of the neutral catalyst changes accordingly. However, in reality, catalysts are usually charged by accepting or donating electrons on the electrode to match the Fermi level (E_F) of the catalyst with the applied electrode potential (μ_e), and the charge usually changes as the reaction proceeds. This leads to the fact that the surface charge effect cannot be captured by the canonical ensemble, and the surface charge effect can only be captured under the grand-canonical ensemble. In 2018, Yuanyue Liu et al. introduced a grand-canonical calculation [24]. Taking common two-dimensional (2D) electrocatalysts and three-dimensional (3D) metal catalysts as examples[14]. The results show that the surface charge has a great influence on the two-dimensional material, which is due to the change of the electronic state occupation caused by the charge [25]. The work of Yuanyue Liu et al. provides a fundamental understanding of charge effects in 2D materials, prompts us to thinking about re-evaluating the previously proposed mechanism, but the work of Yuanyue Liu et al. ignores the variable H coverage, as the H coverage changes, both the surface charge number and the free energy change. In this work, taking 1T'-MoS_2 as an example, we further consider the relationship between surface H coverage and surface charge and ΔG_H under the grand-canonical ensemble.

In addition to focusing on the changes in thermodynamic, we also need to re-evaluate hydrogen evolution mechanism under the grand-canonical ensemble. The search for a self-consistent canonical transition state (TS) under the grand-canonical ensemble is still a challenge due to the difficulty in convergence of electronic iterations. In 2018, Goddard III et al. proposed a grand-canonical potential dynamics model (GCP-K), proving that a grand-canonical process can be simulated by canonical computation using quadratic grand-canonical potential, since it can determine the spatial reaction coordinates as well as the surface charge, which provides a theoretical basis for exploring practical approaches[26]. Completely different from the traditional Butler-Volmer description, each system maintains an integer number of electrons, for grand-canonical potential dynamics, the system transitions to the product by tunneling between the electrode and the reacting molecule. Taking 1T'-MoS_2 as an example, we further verified the effect of surface charge on reaction kinetics by using the GCP-K model.

2. Models and Methods

2.1. Model system

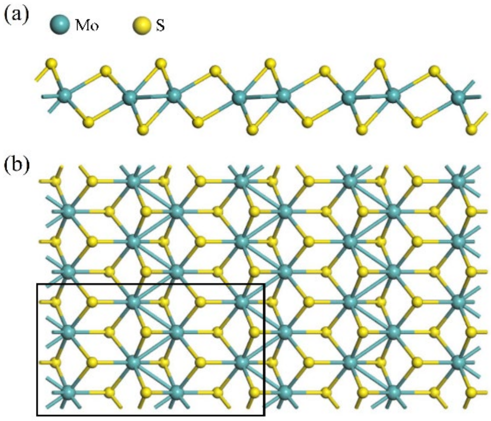

Figure 1: Side view (a) and top view (b) of the single-layer 1T'-MoS_2.

The 1T'-MoS_2 single-layer model was choosed for the thermodynamic calculation, it has 8 MoS_2 formula units (f.u.). Affected by the Charge Density Wave (CDW) [27, 28] caused by the strong coulomb interaction between Mo atoms, the Mo atoms on the surface of the MoS_2 monolayer are distributed in a zigzag shape. The calculation model is shown in Figure 1. S atoms are differentiated into two types of positions with different heights: one type is fixed on the zigzag line of Mo atom, which is higher in the direction of the vacuum layer, and the other type of S atom is located between the two zigzag lines, and its position along the direction of the vacuum layer is lower than the former type.

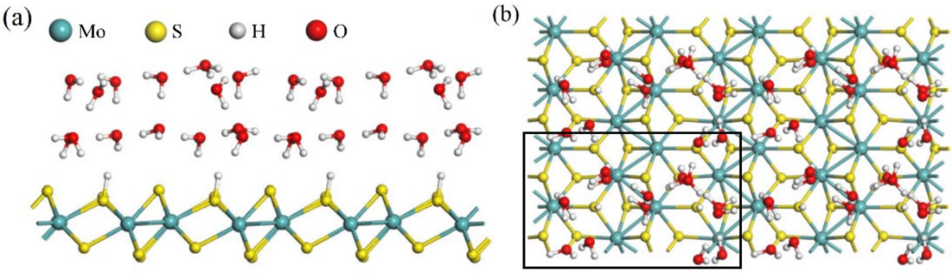

The 1T'-MoS2 basal plane contains two kinds of S atoms with different heights in (a). The 2 × 2 supercell in the rectangular box in (b) is the calculated cell size selected in this work, including 8 MoS2 molecules and 14 H2O molecules.

Figure 2: Side view (a) and top view (b) of the 1T'-MoS2/H2O electrochemical double layer (EDL).

The research on the reaction mechanism of the 1T'-MoS_2 basal plane adopts the electric double layer model, which means adding a water layer on the upper side of the catalyst to build a solid-liquid interface model. As shown in Figure 2, the supercell used in the calculation is a 2×2 supercell unit, which contains 8 MoS_2 molecules and 14 water molecules. Similar to the monolayer 1T'-MoS_2, under the influence of CDW[27, 28], the Mo atoms on the surface of the MoS_2 monolayer are distributed in a zigzag shape, and the S atoms are therefore differentiated into two types of positions with different heights.

2.2. Canonical calculations

The DFT calculation was performed using the Vienna Ab initio Simulation Package (VASP) with the projector augmented wave (PAW) potential[29-31]. The generalized-gradient approximation (GGA) [32]parameterized by the Perdew-Burke-Ernzerhof (PBE) method was chosen as the exchange correlation function for the simple hydrogen adsorption model (without water molecular layer). The optB86b exchange correlation function was used to describe van der Waals (vdW) interactions[33-35]. Using a Monkhorst-Pack grid with 0.02 Å spacing and a cutoff energy of 500 eV. All structures were relaxed until the forces on atoms were smaller than 0.02 eV/Å. Dynamics calculation uses the Climbing Image Nudged Elastic Band (CI-NEB) method to locate the transition state structure [36-41].

2.3. Grand-canonical total energy calculations

Grand-canonical total energy calculations were performed by JDFTx code with CANDLE solvation model [42,43]. This package was developed for self-consistent fixed-potential calculations of electrochemical systems. In order to facilitate the comparison with the canonical calculation results, its calculation parameters, such as exchange correlation function, cut-off energy and convergence criteria, are consistent with that of the VASP.

2.4. Grand-canonical calculations of TS

We use the GCP-K model developed by Goddard III et al.[26] to calculate the potential barriers for the Heyrovsky and Volmer reactions of 1T'-MoS_2.

3. Results and Discussions

3.1. Surface charge affects thermodynamic properties

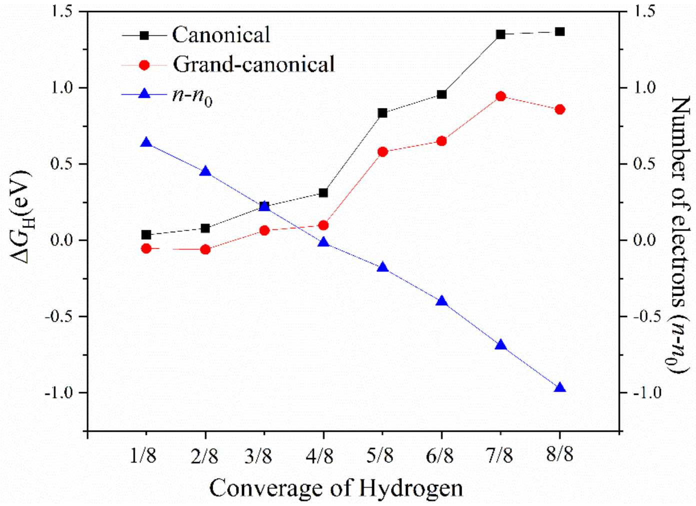

Figure 3: The corresponding hydrogen adsorption energies (ΔG_H) of monolayer 1T'-MoS_2 under different H coverage were calculated by Jdftx. The black square is the canonical calculation result, the red solid circle is the grand-canonical calculation result, and the blue triangle is the difference between the total number of electrons and the number of neutral electrons ($n - n_0$).

The hydrogen adsorption energy (ΔG_H) has been used as a thermodynamic descriptor to characterize the HER activity of catalysts, and previous theoretical and experimental studies have shown that the maximum H coverage corresponds to a ΔG_H of about 0.2 eV [44-46], we use this as a criterion for H coverage. We use the JDFTx package with the CANDEL solvation model for grand-canonical free energy calculations, and obtained the relationship between the H coverage of the monolayer 1T'-MoS_2 basal plane and ΔG_H and surface charge. As shown in Figure 3, the ΔG_H of monolayer 1T'-MoS_2 increases with H coverage. The best HER activity corresponds to the H coverage of 3/8, the ΔG_H calculated by the grand-canonical calculation is 0.064 eV, while the ΔG_H calculated by the canonical calculation is higher, about 0.22 eV. At the same time, through the grand-canonical calculation results, we found that under the standard SHE potential, when the H coverage increased from 3/8 to 4/8, the total charge of the system changed from losing electrons to gaining electrons. These results all prove that the surface charge effect does have a great influence on the thermodynamic calculation.

3.2. Surface charge effects affect kinetic properties

We also used the GCP-K model developed by Goddard III et.al. to calculate the barriers of the Volmer reaction and the Heyrovsky reaction. Herein, we present a detailed computational process for the latter.

According to the GCP-K model, the grand-canonical potential can be obtained by calculating and fitting the constant charge free energy $F(n)$ as a function of the electron number n. Here, $F(n)$ is calculated by using the JDFTx code with the CANDEL solvation model. The result for the IS structure is shown in Figure 4.

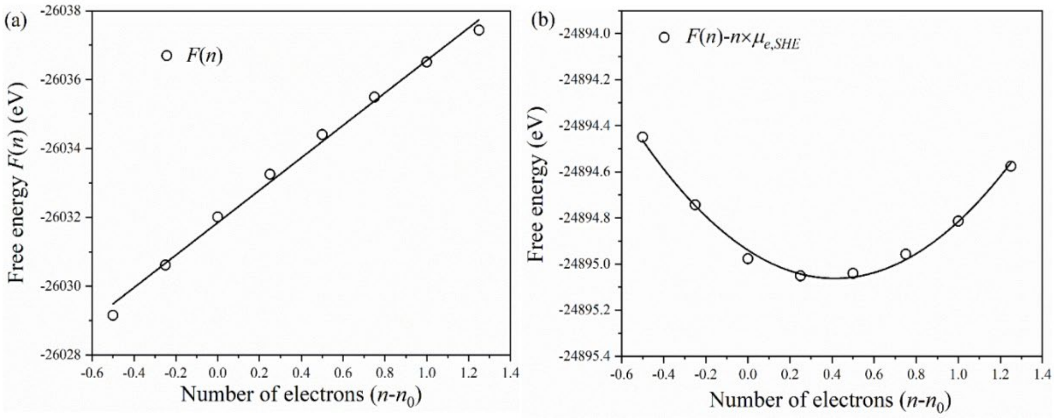

(a) A linear fitting to F(n) *(b) A quadratic fitting to F(n)-n×$\mu_{e,\ SHE}$.*

Figure 4: Free energy and grand-canonical potential as a function of the number of electrons for the IS structure. The DFT energy are indicated by black dots, and the black curve indicates the polynomial fit.

Due to the large contribution of electron energy under SHE conditions (*i.e.* $\mu_{e,SHE}$ = 4.66 eV for the CANDEL method in JDFTx), the $F(n)$ curve does not exhibit the quadratic dependence predicted by the model. By subtracting the contribution of $n\times\mu_{e,SHE}$, we get the grand-canonical energy $G(n, U = 0V) = F(n) - n\times\mu_{e,SHE}$ at 0V, as shown in Figure 4b, the curve has a clear quadratic dependence, the minimum of the curve determines the grand-canonical free energy of the IS at the SHE condition $G_{IS,\ SHE}$ = -24526.92 eV. By fitting the GCP-K curve, we can obtain the net surface charge of the initial state structure n_{SHE} = 0.41. In a similar way, we get the grand-canonical free energy $G_{FS,\ SHE}$ = -24526.73 eV, corresponding to $n_{FS,\ SHE}$ = 0.76.

The grand-canonical free energie of TS ($G_{TS,\ SHE}$) was calculated in a similar way. First, we used the constant-charge CI-NEB method to localize TS structure with different n. Then, the $F(n)$ of the structure was calculated by using the CANDLE solvation model and the results are shown in Figure 5.

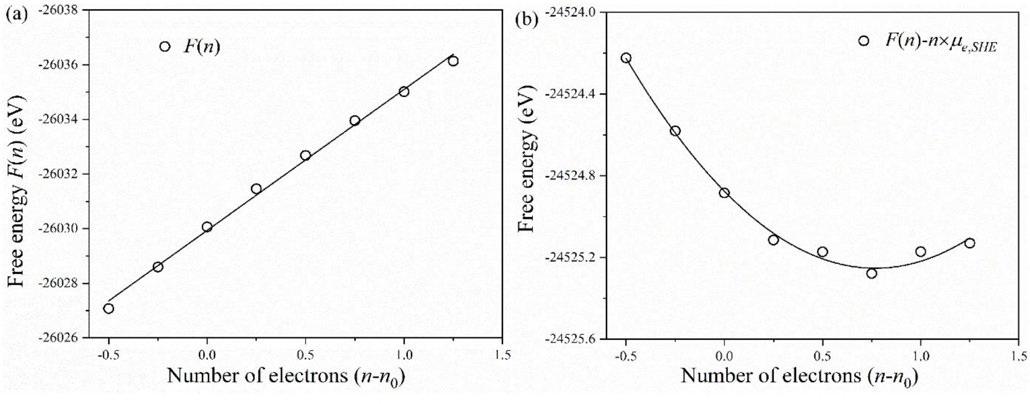

(a) A linear fitting to F(n) *(b) A quadratic fitting to F(n)-n×$\mu_{e,\ SHE}$.*

Figure 5: Free energy and grand-canonical potential as a function of the number of electrons for the TS structure. The DFT energy are indicated by black dots, and the black curve indicates the polynomial fit.

From the minimum of the $G(n, U = 0\text{V})$ curve, we get $G_{\text{TS, SHE}}$ = -24525.25 eV. The grand-canonical barrier $\Delta G^{\ddagger} = G_{\text{TS, SHE}} - G_{\text{IS, SHE}}$ = 1.67 eV, and by fitting the GCP-K curve, we obtain that the net surface charge n_{SHE} of the transition state structure is about 0.77, compared with the net surface charge of the initial state (n_{SHE}= 0.41), we can find that along the reaction path, the electrons are gradually injected.

In a similar way, the $n_{\text{IS, SHE}}$ of the Volmer reaction was calculated to be 0.42, 0.25 for $n_{\text{TS, SHE}}$, 0.28 for $n_{\text{IS, SHE}}$, and the number of electrons gradually decreased along the reaction path. The grand-canonical barrier of the Volmer reaction is 0.26 eV, which is much smaller than that of the Heyrovsky reaction. This result is consistent with the previous canonical calculation. The Heyrovsky barrier obtained in the canonical calculation is about 1.45 eV and the Volmer barrier is about 0.43 eV[45], confirming that the rate-determining step (RDS) is the desorption step.

The two methods give very similar results, but the Heyrovsky reaction barrier calculated by GCP-K is larger than the canonical result while the Volmer barrier is smaller. This may be due to the surface charge effect. Along the reaction route, electrons keep flowing into the catalyst, which can have two effects: (1) the decrease in the electron chemical potential μ_e under the canonical ensemble leads to a decrease in the canonical energy. (2) μ_e is boosted to match $\mu_{e,\text{ SHE}}$ under the grand-canonical ensemble. In this case, the more electrons are added, the higher the energy. If we consider the whole reaction process, there may be more electrons flowing into the catalyst, for the Volmer reaction, mainly the first case affects the energy of the TS, only 0.17 electrons are reduced from the reactant to the saddle point. However, for the Heyrovsky reaction, it suffers more from the second case due to the addition of more SHE electrons (0.35). This explains the opposite changes in the reaction barriers for Volmer and Heyrovsky.

4. Conclusions

In this work, we used the JDFTx software package with the CANDEL solvation model, taking the single-layer 1T'-MoS_2 as the computational model to perform a thermodynamic analysis of the hydrogen evolution reaction under the grand-canonical ensemble and re-evaluating the surface H coverage. We found that for the same material, different H coverages were obtained by the grand-canonical calculation and the canonical calculation respectively, and the difference between the two methods increased with H coverage. At the same time, with the increase of H coverage, the system gradually loses electrons and the hydrogen adsorption energy increases. This shows that the surface charge does have a great influence on the thermodynamics of the reaction.

Meanwhile, we re-evaluate the Heyrovsky and Volmer reaction on the 1T'-MoS_2 basal plane by simulating the real catalytic environment by using the GCP-K model. We found that the Heyrovsky reaction process gradually injects electrons, while the Volmer reaction process gradually loses electrons. Through calculation, we found that the reaction rate-limiting step predicted by the GCP-K model is the desorption step, which is consistent with the regularization, but the reaction barrier is different, mainly because the surface charge affects the reaction barrier.

Acknowledgements

The high-performance computing platform of Jinan University is thanked for providing computational support.

References

[1] Turner J A. Sustainable hydrogen production [Z]. Science. 2004: 972-4.10.1126/science. 1103197
[2] Lewis N S, Nocera D G. Powering the planet: Chemical challenges in solar energy utilization [R], 2006.
[3] Chu S, Majumdar A. Opportunities and challenges for a sustainable energy future [Z]. Nature. 2012: 294-303.10.1038/nature11475
[4] Voiry D, Yamaguchi H, Li J, et al. Enhanced catalytic activity in strained chemically exfoliated WS2 nanosheets for hydrogen evolution [J]. Nature materials, 2013, 12(9): 850-5.
[5] Gong M, Zhou W, Tsai M C, et al. Nanoscale nickel oxide/nickel heterostructures for active hydrogen evolution electrocatalysis [J]. Nature Communications, 2014, 5.
[6] Morales-Guio C G, Stern L A, HU X. Nanostructured hydrotreating catalysts for electrochemical hydrogen evolution [Z]. Chemical Society Reviews. Royal Society of Chemistry. 2014: 6555-

69.10.1039/c3cs60468c

[7] Kibler L A. Hydrogen electrocatalysis [Z]. ChemPhysChem. Wiley-VCH Verlag. 2006: 985-91.10.1002/cphc.200500646

[8] Gaa I E, Hohenbergt Ecole P, Superzeure I A X, et al. Physical ReviEW [R], 2005.

[9] Gritsenko O V, Baerends E J. The spin-unrestricted molecular Kohn-Sham solution and the analogue of Koopmans's theorem for open-shell molecules [J]. Journal of Chemical Physics, 2004, 120(18): 8364-72.

[10] Ramapraba P S, Rama Kishore S, Jayanthi S, et al. The energy density functional formalism for excited states You may also like Shift Learning by Integrating Image and Subsystem Training for Edge Detection in Medical Images Detection of Motorcycle Theft Using Force Sensing Resistor and Ultrasonic Sensor The energy density functional formalism for excited states [R]. 1979.

[11] Greeley J, Jaramillo T F, Bonde J, et al. Computational high-throughput screening of electrocatalytic materials for hydrogen evolution [J]. Nature Materials, 2006, 5(11): 909-13.

[12] Greeley J, Mavrikakis M. Alloy catalysts designed from first principles [J]. Nature Materials, 2004, 3(11): 810-5.

[13] SKúLason E, Tripkovic V, Björketun M E, et al. Modeling the electrochemical hydrogen oxidation and evolution reactions on the basis of density functional theory calculations [J]. Journal of Physical Chemistry C, 2010, 114(42): 18182-97.

[14] Nørskov J K, Bligaard T, Logadottir A, et al. Trends in the Exchange Current for Hydrogen Evolution [J]. Journal of The Electrochemical Society, 2005, 152(3): J23-J.

[15] Parsons R. The rate of electrolytic hydrogen evolution and the heat of adsorption of hydrogen [J]. Transactions of the Faraday Society, 1958, 54: 1053-63.

[16] Conway B E, Tilak B V. Interfacial processes involving electrocatalytic evolution and oxidation of H2, and the role of chemisorbed H [R]. 2002.

[17] Faber M S, Jin S. Earth-abundant inorganic electrocatalysts and their nanostructures for energy conversion applications [Z]. Energy and Environmental Science. Royal Society of Chemistry. 2014: 3519-42.10.1039/c4ee01760a

[18] Wang H, Lu Z, Xu S, et al. Electrochemical tuning of vertically aligned MoS2 nanofilms and its application in improving hydrogen evolution reaction [J]. Proceedings of the National Academy of Sciences of the United States of America, 2013, 110(49): 19701-6.

[19] Barber J, Morin S, Conway B E. Specificity of the kinetics of H 2 evolution to the structure of single-crystal Pt surfaces, and the relation between opd and upd H [R]. 1998.

[20] Kunimatsu K, Senzaki T, Tsushima M, et al. A combined surface-enhanced infrared and electrochemical kinetics study of hydrogen adsorption and evolution on a Pt electrode [J]. Chemical Physics Letters, 2005, 401(4-6): 451-4.

[21] Markovic N M, Ross P N. Surface science studies of model fuel cell electrocatalysts [R]. 2002.

[22] Markovic´ N M M, Grgur B N, Ross P N. Temperature-Dependent Hydrogen Electrochemistry on Platinum Low-Index Single-Crystal Surfaces in Acid Solutions [R]. 1997.

[23] Tavares M C, Machado S A S, Mazo L H. Study of hydrogen evolution reaction in acid medium on Pt microelectrodes [R]. 2001.

[24] Sundararaman R, Goddard W A, Arias T A. Grand canonical electronic density-functional theory: Algorithms and applications to electrochemistry [J]. Journal of Chemical Physics, 2017, 146(11).

[25] Kim D, Shi J, Liu Y. Substantial Impact of Charge on Electrochemical Reactions of Two-Dimensional Materials [J]. Journal of the American Chemical Society, 2018, 140(29): 9127-31.

[26] Huang Y, Nielsen R J, Goddard W A. Reaction Mechanism for the Hydrogen Evolution Reaction on the Basal Plane Sulfur Vacancy Site of MoS 2 Using Grand Canonical Potential Kinetics [J]. Journal of the American Chemical Society, 2018, 140(48): 16773-82.

[27] Shen D W, Xie B P, Zhao J F, et al. Novel mechanism of a charge density wave in a transition metal dichalcogenide [J]. Physical Review Letters, 2007, 99(21).

[28] Zhu Z, Cheng Y, Schwingenschlögl U. Origin of the charge density wave in 1T-TiSe 2 [J]. Physical Review B - Condensed Matter and Materials Physics, 2012, 85(24).

[29] Blochl P E. Projector augmented-+rave method [R]. 1994.

[30] Dal Corso A, Pasquarello A, Baldereschi A, et al. Generalized-gradient approximations to density-functional theory: A comparative study for atoms and solids [R]. 1996.

[31] Kresse G, Joubert D. From ultrasoft pseudopotentials to the projector augmented-wave method [R]. 1999.

[32] Perdew J P, Burke K, ErnzerhoF M. Generalized gradient approximation made simple [J]. Phys Rev Lett, 1996, 77(18): 3865.

[33] DION M, RYDBERG H, SchrödER E, et al. Van der Waals density functional for general geometries [J]. Physical Review Letters, 2004, 92(24).

[34] Román-Pérez G, SoleR J M. Efficient implementation of a van der waals density functional: Application to double-wall carbon nanotubes [J]. Physical Review Letters, 2009, 103(9).

[35] Klime J, Bowler D R, Michaelides A. Van der Waals density functionals applied to solids [J]. Physical Review B - Condensed Matter and Materials Physics, 2011, 83(19).

[36] Sheppard D, Xiao P, Chemelewski W, et al. A generalized solid-state nudged elastic band method [J]. J chem phys, 2012, 136(7): 074103.

[37] Sheppard D, Henkelman G. Paths to which the nudged elastic band converges [J]. J Comput Chem, 2011, 32(8): 1769-71.

[38] Sheppard D, Terrell R, Henkelman G. Optimization methods for finding minimum energy paths [J]. J chem phys, 2008, 128(13): 134106.

[39] JóNSSON H, Mills G, Jacobsen K W. Nudged elastic band method for finding minimum energy paths of transitions [J]. 1998.

[40] Henkelman G, Uberuaga B P, JóNsson H. A climbing image nudged elastic band method for finding saddle points and minimum energy paths [J]. J chem phys, 2000, 113(22): 9901-4.

[41] Henkelman G, Jónsson H. Improved tangent estimate in the nudged elastic band method for finding minimum energy paths and saddle points [J]. J chem phys, 2000, 113(22): 9978-85.

[42] Sundararaman R, Goddard W A. The charge-asymmetric nonlocally determined local-electric (CANDLE) solvation model [J]. Journal of Chemical Physics, 2015, 142(6).

[43] Sundararaman R, Letchworth-Weaver K, Schwarz K A, et al. JDFTx: Software for joint density-functional theory [J]. SoftwareX, 2017, 6: 278-84.

[44] Zeng H, Chen S, Jin Y Q, et al. Electron Density Modulation of Metallic MoO2by Ni Doping to Produce Excellent Hydrogen Evolution and Oxidation Activities in Acid [J]. ACS Energy Letters, 2020, 5(6): 1908-15.

[45] Chen S, Chen X, Wang G, et al. Reaction Mechanism with Thermodynamic Structural Screening for Electrochemical Hydrogen Evolution on Monolayer 1T' Phase MoS_2 *[J]. Chemistry of Materials, 2018, 30(15): 5404-11.*

[46] Tang Q, Jiang D E. Mechanism of hydrogen evolution reaction on 1T-MoS_2 *from first principles [J]. ACS Catalysis, 2016, 6(8): 4953-61.*